Check for updates

Original Research Article

Curcumin Loaded with Ferric Oxide Nanoparticles Reduces Hypoxic Injury in Myocardial Infarction by Regulating miR-208 and Activating SIRT1 Signaling Pathway

Pharmacognosy Magazine
22(4) 1321–1333, 2026
© The Author(s) 2025
Article reuse guidelines:
in.sagepub.com/journals-permissions-india
DOI: 10.1177/09731296251388232
journals.sagepub.com/home/phm
Sage

Dandan Wei[1] and Lei Zhao[2]

Abstract

Background: Curcumin has antioxidant and anti-myocardial ischemic effects, but its low water solubility and bioavailability limit clinical application.

Objectives: This study aims to explore whether curcumin-loaded ferric oxide nanoparticles alleviate hypoxic injury in myocardial infarction.

Materials and Methods: Preparation of ferric oxide (Fe_3O_4) nanoparticle-loaded curcumin complex. A cardiomyocyte hypoxia model was established using ligation surgery. The complex, Fe_3O_4 nanoparticles, and curcumin were applied to the hypoxia model, respectively, and a blank control group was established. The expression of microRNA-208 (miR-208) in cells in each group was detected by fluorescence quantitative polymerase chain reaction. Western blot was used to detect the expression of sirtuin 1 (SIRT1), p53, and hypoxia-inducible factor 1-alpha proteins in cells in each group. The cell counting kit-8 was used to detect cell proliferation in each group.

Results: The Fe_3O_4 nanoparticle-loaded curcumin complex was successfully prepared, and the myocardial infarction rat model was successfully constructed. *In vivo* experimental results show that Fe_3O_4 nanoparticles loaded with curcumin complex can significantly reduce the expression level of miR-208 and increase the activity of SIRT1. After hypoxic treatment of myocardial cells, adding composite nanoparticles can reduce cell damage, reduce the cell apoptosis rate, significantly reduce the size of myocardial infarction, and improve myocardial function, and the effect is stronger than curcumin alone.

Conclusion: Fe_3O_4 nanoparticles loaded with curcumin activate the SIRT1 signaling pathway by downregulating miR-208, and inhibit the expression of p53 and HIF-1α, and ultimately reduce hypoxic injury in myocardial infarction. This provides new ideas and methods for the treatment of myocardial infarction.

Keywords

Ferric oxide nanoparticles, curcumin, miR-208, SIRT1, myocardial infarction

Received 20 January 2025; **revised** 21 May 2025; **accepted** 18 September 2025

Introduction

In myocarditis, curcumin can promote the expression of Beclin-1 (Feng et al., 2019), thereby promoting myocardial autophagy activity, significantly reducing the expression of interleukin-1 beta (IL-1β) and Inos (Li et al., 2022), and significantly increasing the expression of MMR and Arg-1 (Cao et al., 2022). high, thereby improving heart function. At the same time, it can also significantly reduce ACE, AT1R messenger ribonucleic acid (mRNA) (Heshmati et al., 2020) and protein expression levels in myocardial tissue, thereby improving cardiac function in rats with chronic heart failure (Yang et al., 2022), and alleviate myocardial ischemia by upregulating HO-1 protein activity and expression. Reperfusion injury. In a study on diabetic rats, Hao et al. (2023) found that curcumin can reduce the expression of Collagen I and Collagen III (Mojtabavi et al., 2023) through the transforming growth factor-beta/mothers against decapentaplegic (TGF-β/Smads) (Yin et al., 2020) signaling pathway, thereby improving myocardial fibrosis in diabetic rats.

[1]Department of Cardiology, Nanjing First Hospital, Nanjing Medical University, Nanjing, Jiangsu, China
[2]Department of Cardiology, Jining First People Hospital, Jining, Shandong, China

Corresponding author:
Dandan Wei, Department of Cardiology, Nanjing First Hospital, Nanjing Medical University, Nanjing, Jiangsu 210006, China.
E-mail: kegumu70@163.com

Creative Commons Non Commercial CC BY-NC: This article is distributed under the terms of the Creative Commons Attribution-NonCommercial 4.0 License (http://www.creativecommons.org/licenses/by-nc/4.0/) which permits non-Commercial use, reproduction and distribution of the work without further permission provided the original work is attributed as specified on the SAGE and Open Access pages (https://us.sagepub.com/en-us/nam/open-access-at-sage).

Curcumin is shown to be effective in treating heart disease. In addition, curcumin also has positive effects on hypoxic injury. It can promote the increase in B-cell lymphoma 2 (Bcl-2) expression in PC12 cells induced by hypoxia and reoxygenation (Tang & Ling, 2019) and inhibit the expression of BCL2-associated X (Bax) and cysteine-aspartic acid protease 3 (Caspase-3) proteins (Ghasemi et al., 2023), thereby protecting cells from damage. Although curcumin has strong benefits in treating heart diseases, its poor water solubility, low stability, and low bioavailability (Kukkemane & Jagota, 2019) make its application very limited. Ferric oxide (Fe_3O_4) nanoparticles (NPs) can not only increase the drug's concentration in water solubility (Wang et al., 2022), improve the stability of the drug, and can also guide the drug to act on the treatment site through magnetic fields (Li et al., 2019), improving the targeting and efficacy of the drug. At the same time, it enhances the antioxidant and anti-inflammatory effects of curcumin. However, it is currently unclear whether curcumin is effective against hypoxic injury in myocardial infarction and its specific mechanism of action, and further research is needed.

For myocardial infarction, microRNA-208 (miR-208) can promote the proliferation of cardiac hypertrophic cardiomyopathy (HCM) cells and inhibit their apoptosis by upregulating the expression of C-C motif chemokine ligand 2 (CCL2), C-X3-C motif chemokine ligand 1 (CX3CL1), and response gene to complement 32 (RGC32) (Zhao et al., 2023). Thereby achieving the effect of protecting myocardial cells. In addition, overexpression of miR-208 can significantly increase the phosphorylation level of Akt and activate the phosphoinositide 3-kinase/protein kinase B (PI3K/Akt) signaling pathway (Lee et al., 2021), thereby inhibiting hypoxia-inducible factor 1-alpha (HIF-1α)-mediated cardiomyocyte apoptosis (Rahnavard et al., 2019) and improving the symptoms of myocardial infarction (MI) (Takai et al., 2021). Although miR-208 plays an important role in improving myocardial infarction, it is unclear whether it is regulated by curcumin and has an effect on ischemic damage caused by myocardial infarction (Rostamzadeh et al., 2023), and further research is still needed. Sirtuin 1 (SIRT1) can deacetylate p21 protein to lose its ability to inhibit cell cycle progression (Xiao et al., 2016), and promote myocardial regeneration after myocardial infarction by regulating the cell cycle, DNA damage response, and apoptosis through various pathways (Boarescu et al., 2019). In myocardial ischemia-reperfusion injury, activation of SIRT1 can promote the expression of nuclear factor erythroid 2-related factor 2 (Nrf2) (Pang et al., 2022) and inhibit the inhibitory effect of Kelch-like ECH-associated protein 1 (Keap1) (Hao et al., 2023), thereby upregulating the expression of antioxidant genes (Yan et al., 2021) and reducing the impact of oxidative stress on cells damage. Although it can protect myocardial cells from oxidative stress damage during myocardial infarction, there are few reports on the mechanism of hypoxic injury, and further research is needed.

This study is dedicated to exploring the protective effect of curcumin loaded on Fe_3O_4 NPs on hypoxic injury in myocardial infarction, and the protective mechanism of curcumin in hypoxic injury in myocardial infarction by regulating the miR-208 and SIRT1 signaling pathways (Wang et al., 2022), providing new strategies and drug targets for the treatment of myocardial infarction.

Materials and Methods

Experimental Materials

Instruments, Reagents, and Animals

Curcumin (purity: ≥98%, batch number: 458-37-7, Shanghai Yuanye Bio); Fe_3O_4 NPs (Dalian Lidi Fluid Control); miR-208 antibody (Shanghai Kemin Bio); SIRT1 activator (Uric (Shanghai) Life Sciences); Cleaved-Caspase-3 antibody (Aibixin (Shanghai) Biotechnology); Bax/Bcl-2 kit (Beijing Shengke Boyuan Biotechnology); PCR primers and kits (Shanghai Caiyou Industrial); ribonucleic acid (RNA) extraction kit (Wuxi Bohe Biotechnology).

Experimental animals: Forty 8-week-old male Sprague–Dawley rats (weighing 220 ± 20 g) (Beijing Weitong Lever), which were raised for 12 h respectively in constant temperature, constant humidity, light, and dark environments.

Construction of a Rat Model of Myocardial Infarction

Forty healthy rats were selected, and five were randomly selected without any treatment as the control group. The remaining rats were anesthetized by intraperitoneal injection of 2% sodium pentobarbital solution, 30 mg/kg. The rat was placed supine with its head and limbs fixed, tracheal intubation, and connected to a ventilator. The respiratory rate was 85 times/min, the tidal volume was 5.0 mL, and the respiratory ratio was 1:2. Disinfect the left chest with iodophor, make a 1 cm longitudinal incision diagonally downward at the 3rd–4th intercostal space on the left side of the left sternum, and bluntly separate the muscles and pleura. Place an expander between the third ribs and use No. 6-0 thread to insert a needle 3 mm below the left atrial appendage with a depth of 1 mm and a width of 3 mm. Ligate the left anterior descending coronary artery and suture the incision. An electrocardiogram (ECG) with an elevated ST segment indicates successful modeling. The rats that were successfully modeled (Pinchi et al., 2019) were randomly divided into seven groups, with five rats in each group (the 48-h survival rate after coronary artery ligation is 85%): The proteins of the cells to be tested were extracted from the cells, placed in the lysis buffer for cell lysis and digestion, and then the total protein concentration in the lysis solution was determined. Then, the protein samples were isolated with 10% sodium dodecyl sulfate-polyacrylamide gel electrophoresis (SDS-PAGE) and

transferred onto the membrane. Finally, the membrane was incubated overnight with the primary antibody at 4°C. The dilution ratio of the primary antibody was: anti-SIRT1 (1:1,000), anti-p53 (1:1,500), and anti-HIF-1α (1:1,000). Wash the membrane with the enzyme-labeled secondary antibody (horseradish peroxidase (HRP) labeling, 1:5,000) and incubate for 1 h. The internal reference glyceraldehyde-3-phosphate dehydrogenase (GAPDH) enhances the detection capability. The rats were sacrificed 48 h after successful modeling, and the cardiac tissues were taken for subsequent tests.

Method

Preparation of Fe_3O_4-Jaranol Nanomaterials

Preparation of Fe3O4 NPs. Weigh 10.9 g $FeSO_4 \cdot 7H_2O$ and 4.0 g $FeCl_3 \cdot 6H_2O$ and dissolve them in 30 mL deionized water. Pour in nitrogen and add 2 mL of hydrazine hydrate while stirring with a mechanical stirrer. Then add 35 mL of concentrated ammonia dropwise to adjust the pH of the solution to 9. After stirring for 30 min, the reaction system was heated to 80°C and aged for 1 h. The reaction was stopped, and a magnet was used for magnetic separation. The supernatant was discarded, and the lower solid was washed with deionized water, then with absolute ethanol, and finally dried in a vacuum dryer. Dry at 60°C for 12 h to obtain Fe_3O_4 NPs.

Preparation of Cur-Fe3O4 NPs. Weigh 4 mg Fe_3O_4 and dissolve it in 4 mL of 1% acetic acid solution. After all Fe_3O_4 is dissolved, adjust the pH value to 5 with 2 mol/L sodium hydroxide (NaOH) solution. Weigh 0.25, 0.5, 0.75, and 1 mg of Cur- and dissolve it in 500 μL anhydrous methanol was added dropwise to the Fe_3O_4 solution at a rate of 20 drops/min. After the dropwise addition is completed, an equal volume of 1 mg/mL tripolyphosphate (TPP) solution (purchased from Sigma–Aldrich, item number T9183, purity ≥95%) is added dropwise, and the cross-linking reaction is stirred for 30 min to prepare Cur-Fe_3O_4 NPs. Filter and store at 4°C. The morphology of Cur-Fe_3O_4 NPs was observed by transmission electron microscope.

Experimental Methods

Determination of Cardiac Output Index and Myocardial Infarction Area in Rats

The rats were sacrificed, the heart was peeled off, washed, and dried with physiological saline, the removed heart was placed in a water-free environment, weighed using an accurate balance, and the weight of the heart was recorded. Place the heart in 10% buffered formalin and fix it for a period of time. Then, remove the heart tissue, gently wipe away the liquid on the surface with a paper towel, and use a scalpel to cut the heart into 2 mm slices. Place the heart slices into a centrifuge tube containing 0.1% 2,3,5-triphenyltetrazolium chloride (TTC) solution, and then incubate them in a constant temperature water bath at 37°C for 40 min until the normal part of the myocardium appears dark red, while the myocardial infarction area cannot be stained and appears white. Using image analysis software or a calculator, measure the area of the myocardial infarction on each slice. The myocardial infarction areas of different slices were summed to obtain the total myocardial infarction area (%). Divide the heart weight by the rat's body weight to obtain the cardiac index (unit: mg/g).

Cell Proliferation

Cells were seeded into a 96-well plate (4×10^3 cells per well), cultured in a humidified incubator for 12 h, and treated in a humidified environment of 37°C and 5% CO_2 for 24 and 48 h. Then discard the culture medium, add 10 μL 3-(4,5-dimethylthiazol-2-yl)-2,5-diphenyltetrazolium bromide (MTT) solution and 100 μL fresh Dulbecco's modified Eagle medium (DMEM), and continue culturing for 4 h. Place it on the floor with low-speed shaking for 10 min to dissolve fully. A microplate reader measures the absorbance.

Apoptosis

After the cells in each group were digested, they were made into a suspension of 1 × 106 mL. After centrifugation and washing with phosphate-buffered saline (PBS), 150 μL of the suspension was mixed with 10 μL of buffer, 5 μL of Annexin V-fluorescein isothiocyanate (FITC) dye, and 5 μL of PI dye. Evenly. Next, the mixture was incubated in the dark for 15 min. After the incubation was completed, the mixture was observed using a flow cytometer.

Gene Expression

Total RNA in the cells was extracted, and then a complementary deoxyribonucleic acid (cDNA) synthesis kit was used to reverse-transcribe the RNA and prepare the corresponding cDNA. This allows analysis by a real-time polymerase chain reaction (PCR) system. All mRNA expression values are presented relative to GAPDH, and relative expression levels were estimated using the $2^{-\Delta\Delta Ct}$ method. Table 1 lists the primers and primer sequences.

Western Blotting (WB) Protein Detection (SOD, MIDA, GSH, Apoptosis-related Protein Bax/Bcl-2, Cleaved-caspase)

The proteins of the cells to be tested were extracted from the cells, placed in the lysis buffer for cell lysis and digestion, and then the total protein concentration in the lysis solution was determined. Then, the protein samples were isolated with 10% SDS-PAGE and transferred onto the membrane. Finally, the membrane was incubated overnight with the primary

Table 1. Real-time Polymerase Chain Reaction (PCR) Primers and Primer Sequences.

Primer		Primer Sequence
Cleaved-caspase-3	Forward primer	5′-TCTTGGCTCTTCTTGTGCC-3′
	Reverse primer	5′-CTTGCCGTCCTAGAAAGCAG-3′
GAPDH	Forward primer	5′-AAAGGGTCATCATCTCCGCC-3′
	Reverse primer	5′-AGTGATGGCATGGACTGTGG-3′

Note: GAPDH: Glyceraldehyde-3-phosphate dehydrogenase.

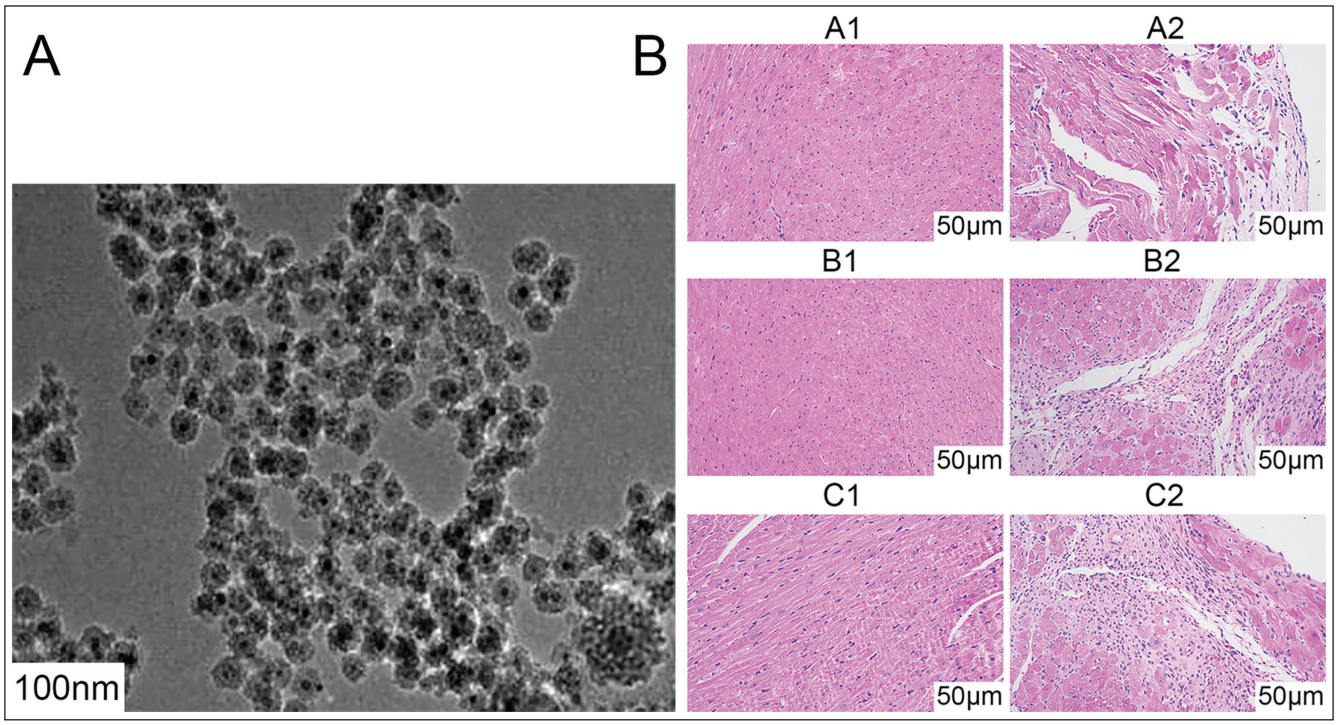


Figure 1. Curcumin-loaded Ferric Oxide Nanoparticles (Cur-Fe_3O_4 NPs) and Myocardial Infarction Rat Model. (A) Cur-Fe_3O_4 NPs Surface; (B) Hematoxylin and Eosin (H&E) Staining Observation.

antibody at 4°C. The dilution ratio of the primary antibody was: anti-SIRT1 (1:1,000), anti-p53 (1:1,500), anti-HIF-1α (1:1,000). Wash the membrane with the enzyme-labeled secondary antibody (HRP labeling, 1:5,000) and incubate for 1 h. The internal reference GAPDH enhances the detection capability.

Statistical Analysis

All data were processed and analyzed using SPSS 21.0 and GraphPad Prism 8.0.2. Data were expressed as mean ± standard deviation. One-way analysis of variance (ANOVA) and Tukey's *post hoc* test were used for multi-group comparisons. Student's *t*-test was used for comparisons between two groups, with $p < .05$ as the test criterion.

Results

Successfully Constructed Cur-Fe_3O_4 NPs and a Myocardial Infarction Rat Model

Fe_3O_4 NPs exhibit a uniform spherical appearance with a particle size of approximately 100 nm (Figure 1A). Curcumin molecules are loaded on the surface of ferro Fe_3O_4 NPs to form a film layer. Through the observation of rat cardiac output index and hematoxylin and eosin (H&E) staining of heart sections, compared with healthy rats, the left ventricular ejection fraction (LVEF) and LVES of rats in the NC group were significantly reduced, and left ventricular end-systolic volume (LVESV) and left ventricular end-diastolic volume (LVEDV) were significantly increased (Figure 1B, Table 2). H&E staining revealed infiltration of inflammatory cells in

Table 2. Observation of Myocardial Infarction Rat Model.

Group	*n*	LVEF (%)	LVFS (%)	LVESV (mL)	LVEDV (mL)
Sham operation group	35	74.06 ± 1.26	38.41 ± 1.09	0.18 ± 0.09	0.52 ± 0.18
Control group	5	35.24 ± 0.24	14.21 ± 0.16	1.24 ± 0.08	1.68 ± 0.15
t Value		67.983	49.032	24.912	13.702
p Value		.000	.000	.000	.000

Note: LVEDV: Left ventricular end-diastolic volume; LVEF: Left ventricular ejection fraction; LVFS: Left ventricular fractional shortening; LVESV: Left ventricular end-systolic volume.

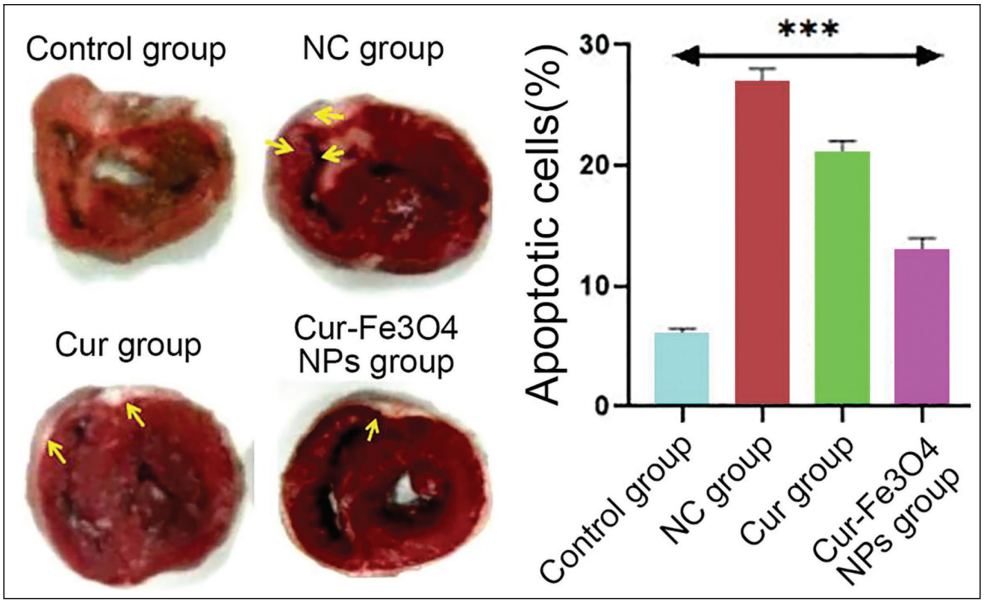


Figure 2. Effect of Curcumin-loaded Ferric Oxide Nanoparticles (Cur-Fe_3O_4 NPs) on Myocardial Infarction Size in Rats.

the slices of the NC group. Myocardial necrosis, cell structure destruction, cell degeneration, fibrosis, and cell nucleus destruction occurred. This shows that the myocardial infarction rat model was successfully constructed.

Effect of Cur-Fe_3O_4 NPs on Hypoxic Injury in Myocardial Infarction

Under the intervention of Cur-Fe_3O_4 NPs, the effect of Apoptotic cells on myocardial infarction size in rats was significantly reduced (Figure 2). Under the intervention of Cur-Fe_3O_4 NPs, the proliferation rate of human cardiomyocyte cell line (AC16) cells increased significantly (Figure 3A, $p < .05$), but the cell apoptosis rate decreased (Figure 3B$p < .05$); and with the intervention of Cur-Fe_3O_4 NPs, the relative expression levels of cleaved-Caspase-3 and Bax/Bcl-2 apoptosis-related proteins decreased (Figure 4A and 4B). With the intervention of Cur-Fe_3O_4 NPs, the superoxide dismutase (SOD) concentration index level increased (Figure 4C), MIDA concentration and glutathione (GSH) concentration indicator levels all showed a decrease (Figure 4D, 4E, and 4F).

Cur-Fe_3O_4 NPs Improve Hypoxic Injury in Myocardial Infarction by Inhibiting miR-208, which is Related to the SIRT1 Signaling Pathway

Under the combined intervention of Cur-Fe_3O_4 NPs and miR-208 inhibitor, the proliferation rate of AC16 cells was alleviated (Figure 5A). Under the combined intervention of Cur-Fe_3O_4 NPs and miR-208 inhibitor, the apoptosis rate of AC16 cells increased (Figure 5B); and in Under the combined intervention of Cur-Fe_3O_4 NPs and miR-208 inhibitor, the relative expression levels of cleaved-Caspase-3 and Bax/Bcl-2 cell apoptosis-related proteins decreased significantly (Figure 5C and 5D); under the combined intervention of Cur-Fe_3O_4 NPs and miR-208 inhibitor, the SOD Concentration and GSH Concentration indicator levels increased (Figure 5E and 5G), the MIDA Concentration indicator level showed a decrease (Figure 5F), and under the combined intervention of Cur-Fe_3O_4 NPs and miR-208 inhibitor, the relative expression increased (Figure 5H). These results indicate that the SIRT1 signaling pathway is involved in the process by which Cur-Fe_3O_4 NPs improve myocardial hypoxic injury.

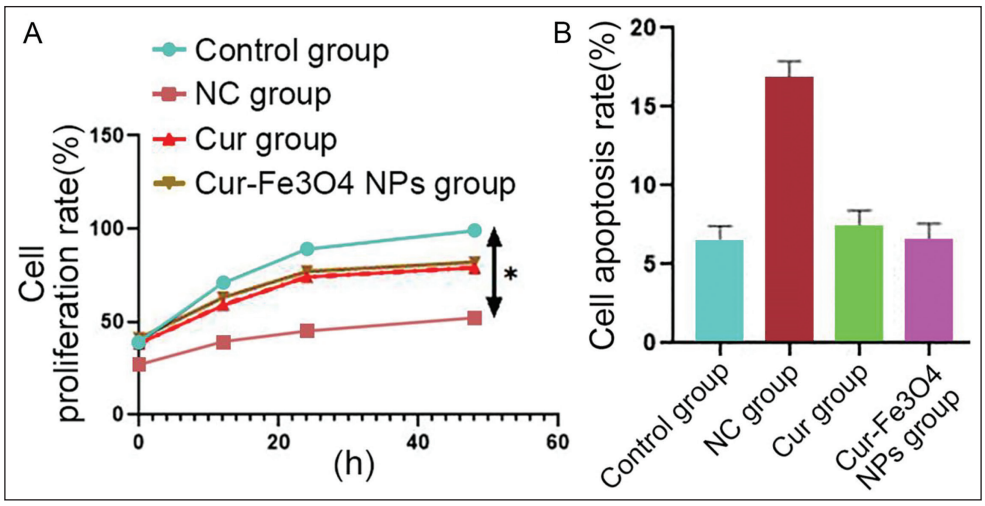


Figure 3. Cell Proliferation and Apoptosis Rate. (A) Cell Proliferation Rate; (B) Cell Apoptosis Rate.

Cur-Fe_3O_4 NPs Can Activate the SIRT1 Signaling Pathway and Alleviate Hypoxic Damage in Myocardial Infarction

Under the joint intervention of Cur-Fe_3O_4 and NPs+SRT1720, the proliferation rate of AC16 cells was alleviated (Figure 6A). Under the joint intervention of Cur-Fe_3O_4 and NPs+SRT1720, the apoptosis rate of AC16 cells was significantly reduced (Figure 6B); in Cur—under the joint intervention of—Fe_3O_4 and NPs+SRT1720, the relative expression levels of cleaved-Caspase-3 and Bax/Bcl-2 cell apoptosis-related proteins decreased significantly (Figure 6C and 6D), and under the joint intervention of Cur-Fe_3O_4 and NPs+SRT1720, the SOD Concentration and GSH Concentration indicator levels showed an increase (Figure 6E and 6G), and the MIDA Concentration indicator level showed a decrease (Figure 6F). It shows that Cur-Fe_3O_4 NPs can activate the SIRT1 signaling pathway and alleviate the hypoxic injury of myocardial infarction.

Cur-Fe_3O_4 NPs Reduce Hypoxic Injury in Myocardial Infarction by Inhibiting miR-208 and Activating the SIRT1 Signaling Pathway

Under the combined intervention of Cur-Fe_3O_4 NPs, miR-208 inhibitor, and SRT1720, the proliferation rate of AC16 cells showed a decline (Figure 7A). Under the combined intervention of Cur-Fe_3O_4 NPs, miR-208 inhibitor and SRT1720, the cell apoptosis rate decreased significantly (Figure 7B); under the combined intervention of Cur-Fe_3O_4 NPs, miR-208 inhibitor and SRT1720, the relative expression levels of cleaved-Caspase-3 and Bax/Bcl-2 cell apoptosis-related proteins were significantly reduced (Figure 7C and 7D), and in Cur-Fe_3O_4 Under the combined intervention of NPs, miR-208 inhibitor and SRT1720, the SOD concentration and GSH concentration indicator levels increased (Figure 7E and 7G), while the MIDA concentration indicator level showed a decrease (Figure 7F). In summary, our experimental results further verify that Cur-Fe_3O_4 NPs activate the SIRT1 signaling pathway by inhibiting miR-208 to alleviate hypoxic injury caused by myocardial infarction. This provides important evidence, support, and guidance for further research and development of relevant treatment strategies.

Discussion

Curcumin itself has low water solubility and oral bioavailability, making it difficult to achieve ideal drug concentrations in the body. As a result, its use is often limited. Curcumin loaded on Fe_3O_4 NPs can increase its water solubility and enhance drug absorption in the digestive tract, thereby increasing the bioavailability of curcumin and enhancing the stability of curcumin (Wang et al., 2021), and helps with the release and targeted delivery of curcumin to cardiomyocytes or injury sites in the body. Based on the above advantages, the Cur-Fe_3O_4 composite was successfully prepared in this experiment. To explore the effect of Cur-Fe_3O_4 NPs on hypoxic injury in myocardial infarction. By observing the proliferation and apoptosis rates of AC16 cardiomyocytes in each group, we found that Cur and Cur-Fe_3O_4 could significantly increase the proliferation rate of cardiomyocytes compared with the control group, with Cur-Fe_3O_4 increasing the most significantly. Similarly, compared with the control group, Cur and Cur-Fe_3O_4 significantly reduced the cardiomyocyte apoptosis rate in cleaved-Caspase-3 and Bax/Bcl-2 ratio in stressed cardiomyocytes, among which the reduction effect of Cur-Fe_3O_4 was the most obvious. It shows that Cur-Fe_3O_4 NPs have a positive effect on improving hypoxic injury in myocardial infarction.

Studies have found that miR-208 inhibits the expression of myosin heavy chain 6 (Myh6) (alpha-myosin heavy chain

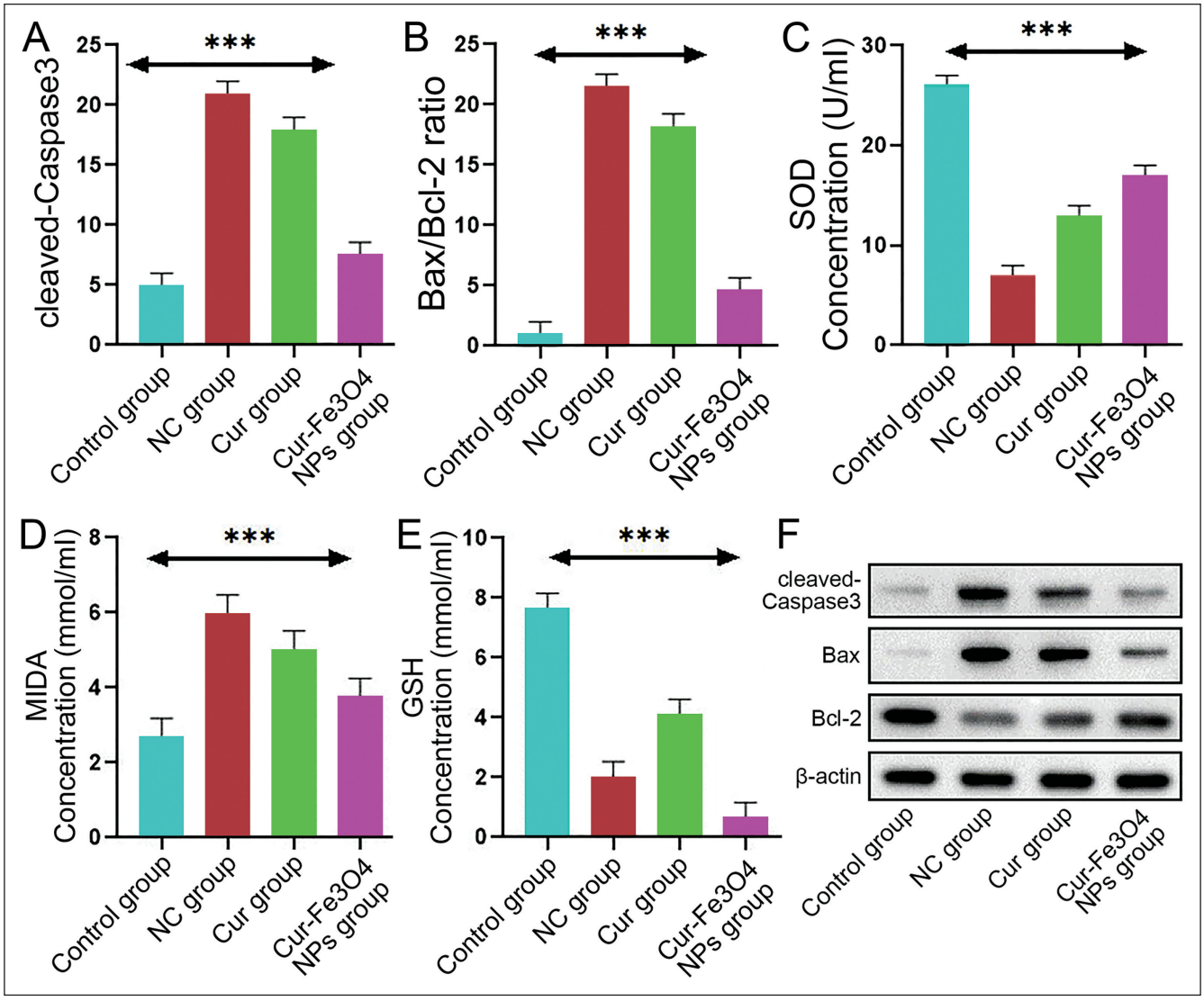


Figure 4. Relative Expression of Cleaved-caspase-3 and Bax/Bcl-2. (A) Cleaved-caspase-3 Apoptosis-related Protein; (B) Bax/Bcl-2 Apoptosis-related Protein; (C) Superoxide Dismutase (SOD) Concentration; (D) MIDA Concentration; (E) Glutathione (GSH) Concentration; (F) Protein Band Diagram.

(α-MHC)) (Paul et al., 2021) and increases the expression of myosin heavy chain 7 (Myh7) (beta-myosin heavy chain (β-MHC)) (Chen et al., 2021), causing cardiomyocytes to change from mature α-MHC type to fetal β-MHC type (Mao et al., 2019), resulting in impairment of myocardial contractility and function. Inhibiting miR-208 can act by increasing the expression of anti-apoptotic proteins (Wei et al., 2021), thus protecting cardiomyocytes from apoptosis damage. Through our research, we found that Cur-Fe_3O_4 NPs improved hypoxic injury in myocardial infarction by inhibiting the expression of miR-208. In experiments, we used agonists and inhibitors of miR-208 to simulate the high and low expression states of miR-208. The results showed that under the intervention of miR-208 mimic, the DNA synthesis rate decreased, the apoptosis rate increased, and the expression of apoptosis-related proteins also increased. Under the intervention of the miR-208 inhibitor, these indicators showed the opposite situation. Next, we observed that the expression of miR-208 was significantly reduced after Cur-Fe_3O_4 NP treatment. This indicates that Cur-Fe_3O_4 NPs can inhibit the expression of miR-208. In further research, we combined the application of Cur-Fe_3O_4 NPs and miR-208 inhibitor and observed that the cell proliferation rate was the highest, the apoptosis rate and the expression of apoptosis-related proteins were the lowest. This shows that Cur-Fe_3O_4 NPs improve hypoxic injury in myocardial infarction by inhibiting the expression of miR-208. In addition, during this process, we also observed that the SIRT1 signaling pathway was activated by the combined treatment of Cur-Fe_3O_4, miR-208 mimic, and Cur-Fe_3O_4 and miR-208 inhibitor. Among them, the

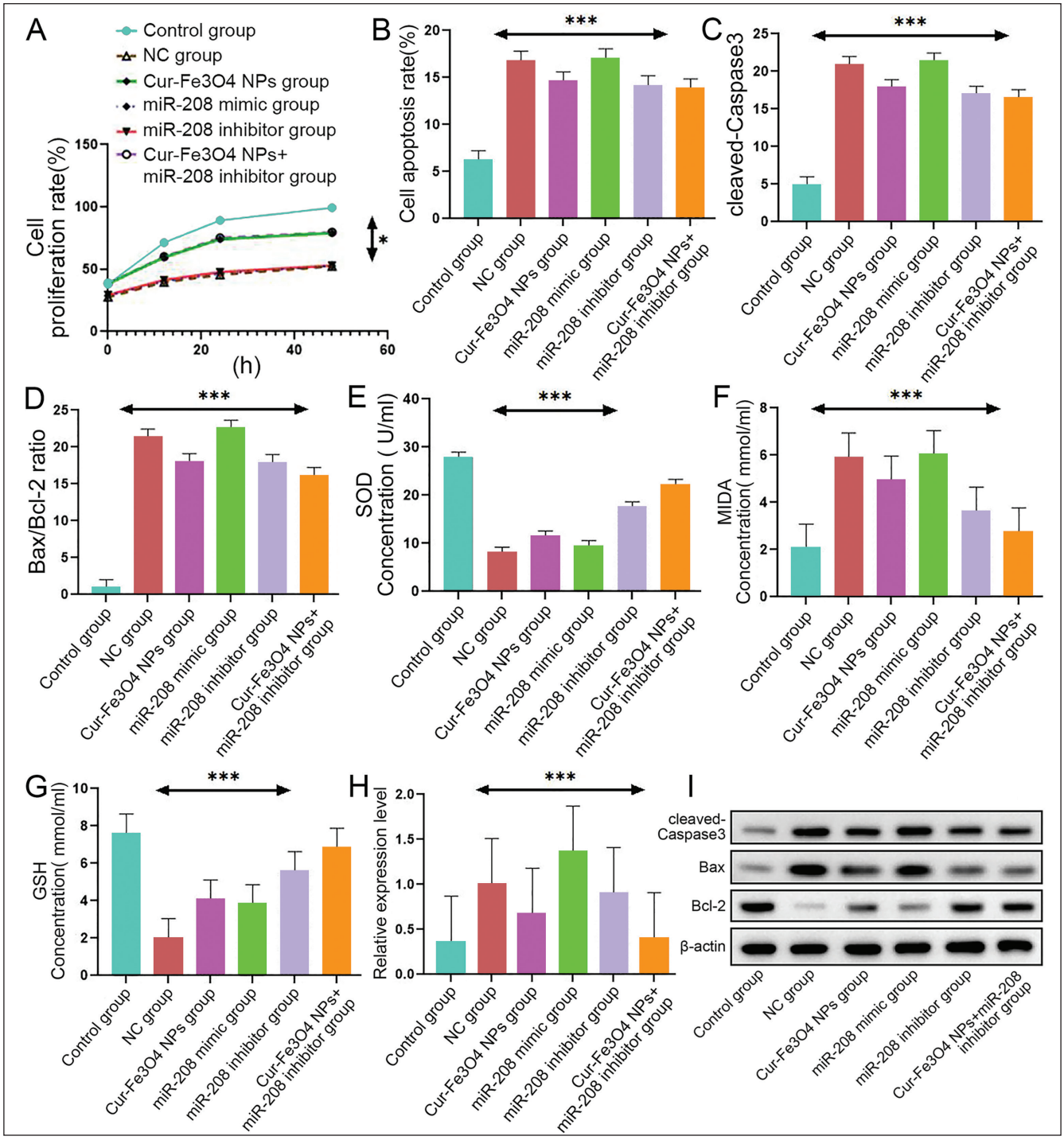


Figure 5. Relative Expression Levels of Cell Apoptosis-related Proteins. (A) Cell Proliferation Rate; (B) Cell Apoptosis Rate; (C) Cleaved-caspase-3 Apoptosis-related Protein; (D) Bax/Bcl-2 Apoptosis-related Protein; (E) Superoxide Dismutase (SOD) Concentration; (F) MIDA Concentration; (G): Glutathione (GSH) Concentration; (H) Relative Expression Level; (I) Protein Band Diagram.

activation effect of the combined treatment of Cur-Fe_3O_4 and miR-208 inhibitor was the most obvious. This indicates that the SIRT1 signaling pathway is involved in the process of Cur-Fe_3O_4 NPs improving hypoxic injury in myocardial infarction by inhibiting miR-208.

Activation of SIRT1 can promote the activation of the AMP-activated protein kinase (AMPK) signaling pathway (Yamac et al., 2019), thereby inhibiting the activity of the apoptosis-inducing factor p53 (Luo et al., 2021) and inhibiting the occurrence of apoptosis. In addition, SIRT1 can inhibit

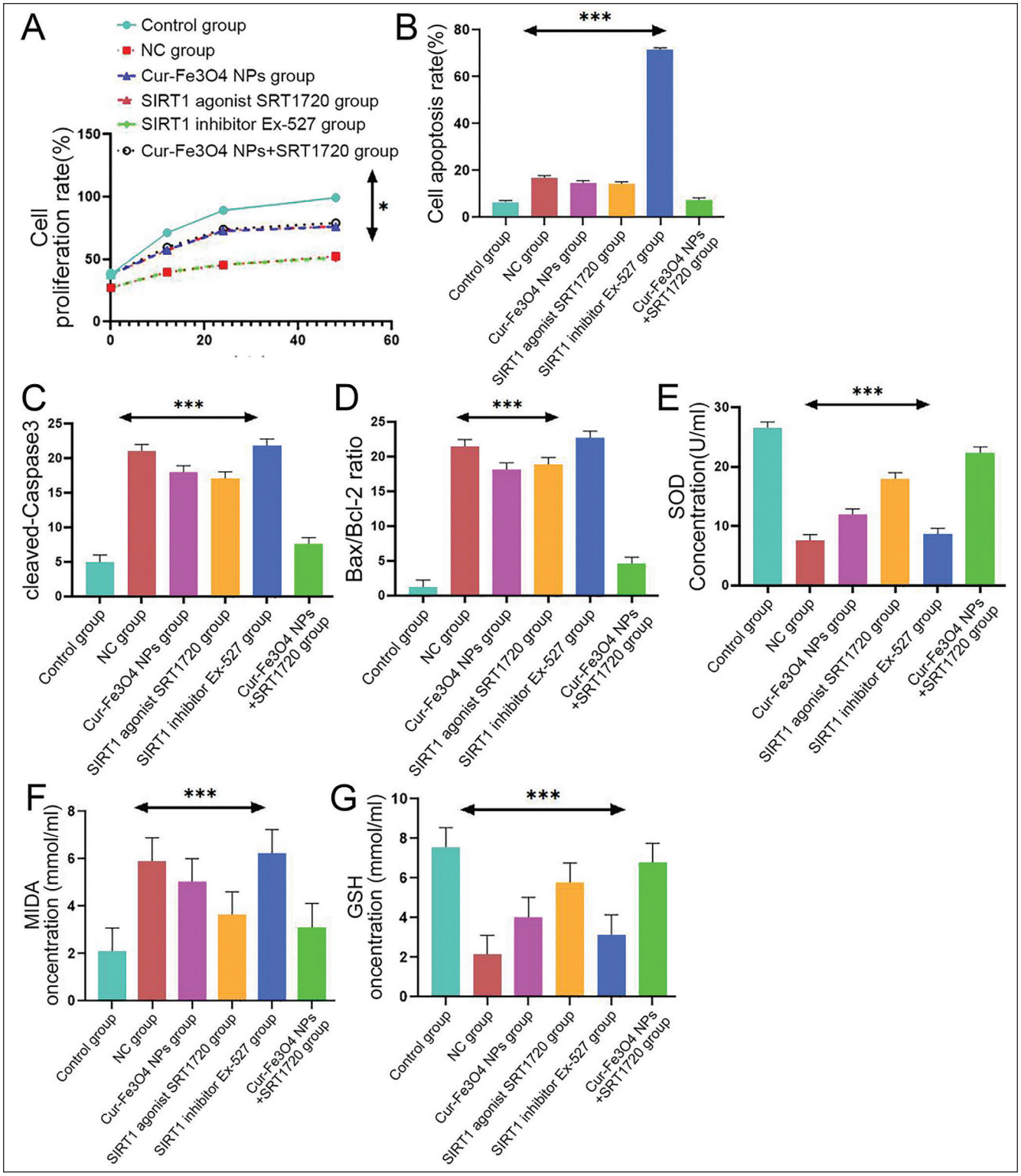


Figure 6. Relative Expression of Apoptotic Proteins. (A) Cell Proliferation Rate; (B) Cell Apoptosis Rate; (C) Cleaved-caspase-3 Apoptosis-related Protein; (D) Bax/Bcl-2 Apoptosis-related Protein; (E) Superoxide Dismutase (SOD) Concentration; (F) MIDA Concentration; (G) Glutathione (GSH) Concentration.

the nuclear factor kappa B (NF-κB) signaling pathway (Xie, 2023) and reduce the production of inflammatory factors such as interleukin-6 (IL-6) and tumor necrosis factor-alpha (TNF-α) (Xu et al., 2023), thereby inhibiting the inflammatory response (Tan et al., 2022) and reducing the degree of inflammatory damage after myocardial infarction. We use

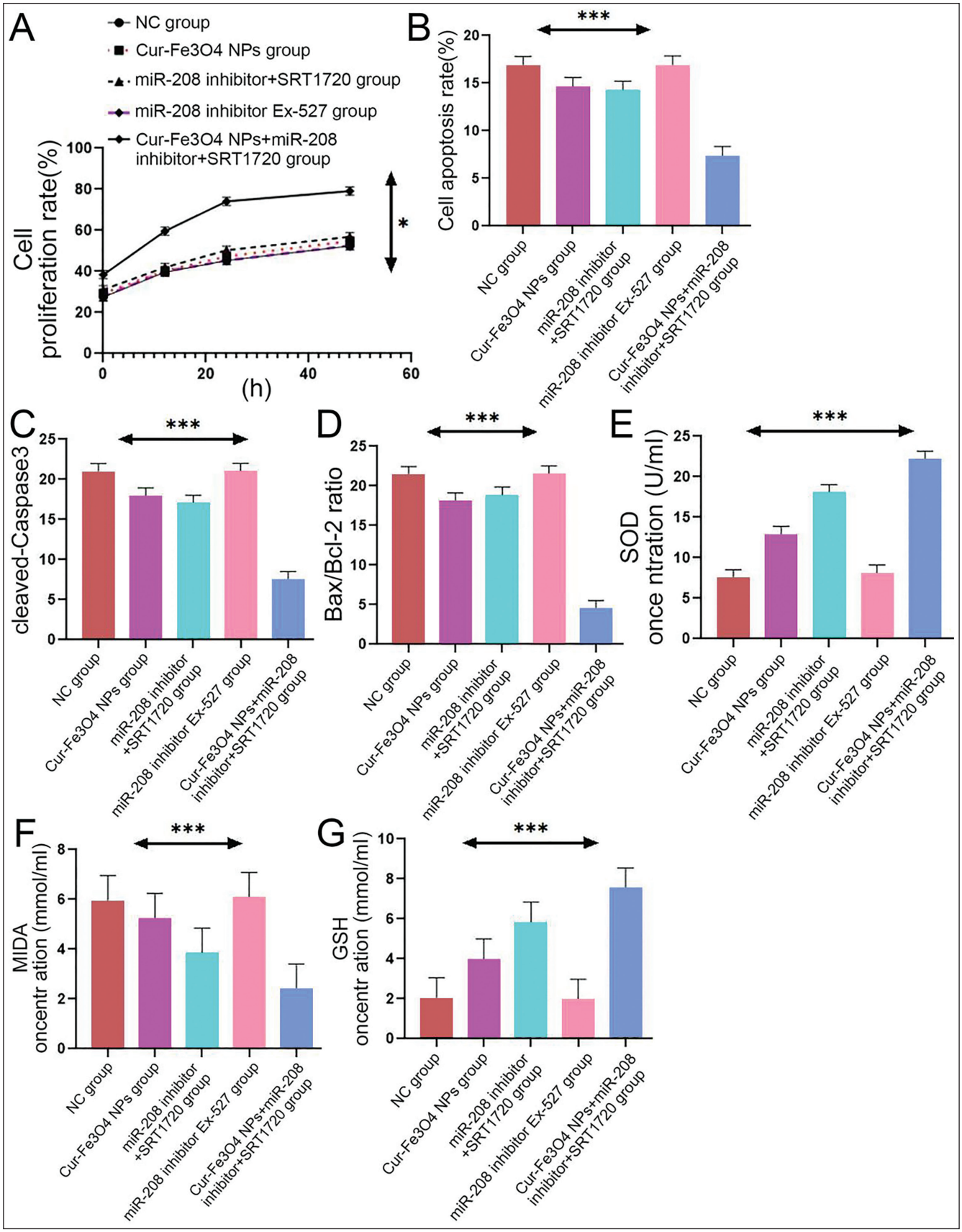


Figure 7. Relative Expression of Cell-related Proteins. (A) Cell Proliferation Rate; (B) Cell Apoptosis Rate; (C) Cleaved-caspase-3 Apoptosis-related Protein; (D) Bax/Bcl-2 Apoptosis-related Protein; (E) Superoxide Dismutase (SOD) Concentration; (F) MIDA Concentration; (G) Glutathione (GSH) Concentration.

two drugs, SRT1720 and SIRT1 inhibitor (Ex-527). The experimental results showed that compared with the control group, the apoptosis rate of AC16 cells treated with SRT1720 was reduced, the proliferation rate was increased, and the expression of apoptosis-related proteins also showed a downward trend. Cells treated with Ex-527 showed the opposite effect. This shows that SRT1720 can promote cell proliferation, reduce apoptosis, and reduce the expression of apoptosis-related proteins. Ex-527 had the opposite effect, inhibiting cell proliferation and increasing the apoptosis rate. In addition, we further conducted experiments on the combined treatment of Cur-Fe_3O_4 NPs and SRT1720 and found that the effect was similar to, or even more significant than, the group using SRT1720 alone. This shows that Cur-Fe_3O_4 NPs can enhance the effect of SRT1720, further promote cell proliferation, reduce the apoptosis rate (Najafipour et al., 2021), and reduce the expression of apoptosis-related proteins. This means that Cur-Fe_3O_4 NPs can alleviate hypoxic damage caused by myocardial infarction by activating the SIRT1 signaling pathway (Liu et al., 2021). Compared with liposomes (such as Doxil® with a drug loading rate of approximately 60%), Fe_3O_4 NPs achieve a curcumin loading rate of over 90% through hydrophobic interactions, and Fe_3O_4 itself can eliminate reactive oxygen species (ROS), jointly enhancing the activation of the SIRT1 pathway with curcumin.

To verify the previous results, we conducted further experiments using a miR-208 inhibitor in combination with SRT1720 and Ex-527. The experimental results showed that compared with the control group, cells treated with miR-208 inhibitor and SRT1720 alone showed similar effects, but the combined effect of miR-208 inhibitor and SRT1720 was more significant. In addition, this effect is further enhanced after adding Cur-Fe_3O_4 NPs. However, miR-208 inhibitor and Ex-527 obviously reversed their previous effects and produced the opposite effect. These results further verify that Cur-Fe_3O_4 NPs activate the SIRT1 signaling pathway by inhibiting miR-208, thereby alleviating hypoxic injury caused by myocardial infarction. By inhibiting miR-208, Cur-Fe_3O_4 NPs can enhance the effect of SRT1720, promote cell proliferation, reduce the apoptosis rate, and reduce the expression of apoptosis-related proteins. The results of the miR-208 inhibitor + Ex-527 group showed that Ex-527 had a significant reverse effect on this effect.

Conclusion

In summary, our experimental results further verify that Cur-Fe_3O_4 NPs activate the SIRT1 signaling pathway by inhibiting miR-208 to alleviate hypoxic injury caused by myocardial infarction. This provides important evidence, support, and guidance for further research and development of relevant treatment strategies. However, there are still certain deficiencies in this study: (a) long-term toxicity experiments were not conducted to verify the safety of NPs; (b) the necessity of further verifying the miR-208/SIRT1 pathway in animals without gene knockout; (c) clinical transformation needs to take into account the dose differences between humans and animals. In the future, the dosing regimens need to be optimized through large animal experiments and clinical trials.

Abbreviations

AC16: Human cardiomyocyte cell line; α-MHC: Alpha-myosin heavy chain; AMPK: AMP-activated protein kinase; ANOVA: Analysis of variance; Bax: BCL2-associated X; Bcl-2: B-cell lymphoma 2; β-MHC: Beta-myosin heavy chain; CCK-8: Cell counting kit-8; CCL2: C-C motif chemokine ligand 2; Caspase-3: Cysteine-aspartic acid protease 3; cDNA: Complementary deoxyribonucleic acid; CO_2: Carbon dioxide; Cur-Fe_3O_4 NPs: Curcumin-loaded ferric oxide nanoparticles; CX3CL1: C-X3-C motif chemokine ligand 1; °C: Degree Celsius; DMEM: Dulbecco's modified Eagle medium; Ex-527: SIRT1 inhibitor; ECG: Electrocardiogram; Fe_3O_4: Ferric oxide; $FeCl_3 \cdot 6H_2O$: Iron(III) chloride hexahydrate; $FeSO_4 \cdot 7H_2O$: Iron(II) sulfate heptahydrate; FITC: Fluorescein isothiocyanate; FOXO3a: Forkhead Box O3a; GAPDH: Glyceraldehyde-3-phosphate dehydrogenase; g: Grams; GSH: Glutathione; H&E: Hematoxylin and eosin; HCM: Hypertrophic cardiomyopathy; HIF-1α: Hypoxia-inducible factor 1-alpha; HRP: Horseradish peroxidase; IL-1β: Interleukin-1 beta; IL-6: Interleukin-6; Keap1: Kelch-like ECH-associated protein 1; LVEDV: Left ventricular end-diastolic volume; LVESV: Left ventricular end-systolic volume; LVEF: Left ventricular ejection fraction; LVFS: Left ventricular fractional shortening; MDA: Malondialdehyde; mg/kg: Milligrams per kilogram; miR-208: microRNA-208; mL: Milliliters; mm: Millimeters; mRNA: Messenger ribonucleic acid; MI: Myocardial infarction; MTT: 3-(4,5-dimethylthiazol-2-yl)-2,5-diphenyltetrazolium bromide; Myh6: Myosin heavy chain 6; Myh7: Myosin heavy chain 7; NaOH: Sodium hydroxide; NF-κB: Nuclear factor kappa B; nm: Nanometers; Nrf2: Nuclear factor erythroid 2-related factor 2; PBS: Phosphate buffered saline; PCR: Polymerase chain reaction; PGC-1α: Peroxisome proliferator-activated receptor gamma coactivator 1-alpha; PI: Propidium iodide; PI3K/Akt: Phosphoinositide 3-kinase/protein kinase B; RGC32: Response gene to complement 32; RNA: Ribonucleic acid; ROS: Reactive oxygen species; Rs: Tumor protein p53; SIRT1: Sirtuin 1; SD: Standard deviation; SDS-PAGE: Sodium dodecyl sulfate-polyacrylamide gel electrophoresis; SOD: Superoxide dismutase; SRT1720: SIRT1 activator; ST: ST Segment; TGF-β/Smads: Transforming growth factor-beta/mothers against decapentaplegic; TNF-α: Tumor necrosis factor-alpha; TPP: Tripolyphosphate; TTC: 2,3,5-Triphenyltetrazolium chloride; WB: Western blotting; μL: Microliters.

Declaration of Conflicting Interests

The authors declared no potential conflicts of interest with respect to the research, authorship, and/or publication of this article.

Ethical Approval and Informed Consent

This study was approved by the ethics committee of Nanjing First Hospital, Nanjing Medical University.

Funding

The authors received no financial support for the research, authorship, and/or publication of this article.

ORCID iD

Dandan Wei https://orcid.org/0009-0007-4589-1731

References

Boarescu, P. M., Chirila, I., Bulboaca, A. E., Bocsan, I. C., Pop, R. M., Gheban, D., & Bolboaca, S. D. (2019). Effects of curcumin nanoparticles in isoproterenol-induced myocardial infarction. *Oxidative Medicine and Cellular Longevity*, *2019*, 7847142. https://doi.org/10.1155/2019/7847142

Cao, Z., Wu, Z., Duan, T., Tang, C., Huang, D., & Hu, X. (2022). Curcumin ameliorates HO-induced injury through SIRT1-PERK-CHOP pathway in pancreatic beta cells. *Acta Biochimica et Biophysica Sinica (Shanghai)*, *54*(3), 370–377. https://doi.org/10.3724/abbs.2022004

Chen, L., Li, S., Zhu, J., You, A., Huang, X., Yi, X., & Xue, M. (2021). Mangiferin prevents myocardial infarction-induced apoptosis and heart failure in mice by activating the Sirt1/FoxO3a pathway. *Journal of Cellular and Molecular Medicine*, *25*(6), 2944–2955. https://doi.org/10.1111/jcmm.16329

Feng, K., Ge, Y., Chen, Z., Li, X., Liu, Z., Li, X., Li, H., Tang, T., Yang, F., & Wang, X. (2019). Curcumin inhibits the PERK-eIF2alpha-CHOP pathway through promoting SIRT1 expression in oxidative stress-induced rat chondrocytes and ameliorates osteoarthritis progression in a rat model. *Oxidative Medicine and Cellular Longevity*, *2019*, 8574386. https://doi.org/10.1155/2019/8574386

Ghasemi, H., Motevali Manesh, S. F., Kheiripour, N., Asl, S. S., Jouzdani, A. F., Ranjbar, A., & Abdolvahab, M. H. (2023). An oxidative stress study on curcumin and nanocurcumin against aluminum phosphide-induced kidney injury in rats: The role of SIRT1/FOXO3 signaling pathway in nephrotoxicity. *Pharmaceutical Nanotechnology*, *12*(5), 449–458. https://doi.org/10.2174/2211738511666230821124704

Hao, H., Yuan, T., Li, Z., Zhang, C., Liu, J., Liang, G., Feng, L., & Pan, Y. (2023). Curcumin analogue C66 ameliorates mouse cardiac dysfunction and structural disorders after acute myocardial infarction via suppressing JNK activation. *European Journal of Pharmacology*, *946*, 175629. https://doi.org/10.1016/j.ejphar.2023.175629

Heshmati, J., Golab, F., Morvaridzadeh, M., Potter, E., Akbari-Fakhrabadi, M., Farsi, F., Tanbakooei, S., & Shidfar, F. (2020). The effects of curcumin supplementation on oxidative stress, Sirtuin-1 and peroxisome proliferator activated receptor gamma coactivator 1alpha gene expression in polycystic ovarian syndrome (PCOS) patients: A randomized placebo-controlled clinical trial. *Diabetes & Metabolic Syndrome*, *14*(2), 77–82. https://doi.org/10.1016/j.dsx.2020.01.002

Kukkemane, K., & Jagota, A. (2019). Therapeutic effects of curcumin on age-induced alterations in daily rhythms of clock genes and Sirt1 expression in the SCN of male Wistar rats. *Biogerontology*, *20*(4), 405–419. https://doi.org/10.1007/s10522-018-09794-y

Lee, G. K., Hsieh, Y. P., Hsu, S. W., & Lan, S. J. (2021). Exploring diagnostic and prognostic predictive values of microRNAs for acute myocardial infarction: A PRISMA-compliant systematic review and meta-analysis. *Medicine (Baltimore)*, *100*(29), e26627. https://doi.org/10.1097/MD.0000000000026627

Li, P., Li, S. Y., Liu, M., Ruan, J. W., Wang, Z. D., & Xie, W. C. (2019). Value of the expression of miR-208, miR-494, miR-499 and miR-1303 in early diagnosis of acute myocardial infarction. *Life Sciences*, *232*, 116547. https://doi.org/10.1016/j.lfs.2019.116547

Li, Y., Luo, W. W., Cheng, X., Xiang, H. R., He, B., Zhang, Q. Z., & Peng, W. X. (2022). Curcumin attenuates isoniazid-induced hepatotoxicity by upregulating the SIRT1/PGC-1alpha/NRF1 pathway. *Journal of Applied Toxicology*, *42*(7), 1192–1204. https://doi.org/10.1002/jat.4288

Liu, C. Y., Zhou, Y., Chen, T., Lei, J. C., & Jiang, X. J. (2021). AMPK/SIRT1 pathway is involved in arctigenin-mediated protective effects against myocardial ischemia-reperfusion injury. *Frontiers in Pharmacology*, *11*, 616813. https://doi.org/10.3389/fphar.2020.616813

Luo, X. Y., Zhong, Z., Chong, A. G., Zhang, W. W., & Wu, X. D. (2021). Function and mechanism of trimetazidine in myocardial infarction-induced myocardial energy metabolism disorder through the SIRT1-AMPK pathway. *Frontiers in Physiology*, *12*, 645041. https://doi.org/10.3389/fphys.2021.645041

Mao, Q., Liang, X. L., Zhang, C. L., Pang, Y. H., & Lu, Y. X. (2019). LncRNA KLF3-AS1 in human mesenchymal stem cell-derived exosomes ameliorates pyroptosis of cardiomyocytes and myocardial infarction through miR-138-5p/Sirt1 axis. *Stem Cell Research & Therapy*, *10*(1), 393. https://doi.org/10.1186/s13287-019-1522-4

Mojtabavi, S., Saed, A., Aboulfazli, S., Kheirandish, A., Najafi, M., Jafari-Sabet, M., Ziar, A., Ebrahimi, N., Mirmajidi, S. H., & Ataee, R. (2023). Evaluation of curcumin effect on Il6, Sirt1, TNFalpha and NFkB expression of liver tissues in diabetic mice with STZ. *Journal of Diabetes & Metabolic Disorders*, *22*(1), 205–215. https://doi.org/10.1007/s40200-022-01090-4

Najafipour, H., Rostamzadeh, F., Yeganeh-Hajahmadi, M., & Joukar, S. (2021). Improvement of cardiac function in rats with myocardial infarction by low-intensity to moderate-intensity endurance exercise is associated with normalization of Klotho and SIRT1. *Journal of Cardiovascular Pharmacology*, *77*(1), 79–86. https://doi.org/10.1097/Fjc.0000000000000935

Pang, B. Y., Wang, Y. H., Ji, X. W., Leng, Y., Deng, H. B., & Jiang, L. H. (2022). Systematic review and meta-analysis of the intervention effect of curcumin on rodent models of myocardial infarction. *Frontiers in Pharmacology*, *13*, 999386. https://doi.org/10.3389/fphar.2022.999386

Paul, A., Pai, P. G., Ariyannur, P. S., & Joy, R. A. (2021). Diagnostic accuracy of MicroRNA 208b level with respect to different types of atrial fibrillation. *Indian Heart Journal*, *73*(4), 506–510. https://doi.org/10.1016/j.ihj.2021.06.018

Pinchi, E., Frati, P., Aromatario, M., Cipolloni, L., Fabbri, M., La Russa, R., Maiese, A., Neri, M., Santurro, A., Scopetti, M., Viola, R. V., Turillazzi, E., & Fineschi, V. (2019). miR-1, miR-499 and miR-208 are sensitive markers to diagnose sudden death due to early acute myocardial infarction. *Journal of Cellular and Molecular Medicine*, *23*(9), 6005–6016. https://doi.org/10.1111/jcmm.14463

Rahnavard, M., Hassanpour, M., Ahmadi, M., Heidarzadeh, M., Amini, H., Javanmard, M. Z., Nouri, M., Rahbarghazi, R., & Safaie, N. (2019). Curcumin ameliorated myocardial infarction by inhibition of cardiotoxicity in the rat model. *Journal of Cellular Biochemistry*, *120*(7), 11965–11972. https://doi.org/10.1002/jcb.28480

Rostamzadeh, F., Jafarinejad-Farsangi, S., Ansari-Asl, Z., Farrokhi, M. S., & Jafari, E. (2023). Treatment for myocardial infarction: *In vivo* evaluation of curcumin-loaded PEGylated-GQD nanoparticles. *Journal of Cardiovascular Pharmacology*, *81*(5), 361–372. https://doi.org/10.1097/FJC.0000000000001410

Takai, H., Sunagawa, Y., Funamoto, M., Shimizu, K., Shimizu, S., Katanasaka, Y., Miyazaki, Y., Imaizumi, A., Hashimoto, T., Wada, H., Hasegawa, K., & Morimoto, T. (2021). A novel curcumin formulation, ASD-cur, suppressed the development of systolic dysfunction after myocardial infarction in rats. *European Cardiology Review*, *16*, e69. https://doi.org/10.15420/ecr.2021.16.PO13

Tan, Y., Bie, Y. L., Chen, L., Zhao, Y. H., Song, L., Miao, L. N., Yu, Y. Q., Chai, H., Ma, X. J., & Shi, D. Z. (2022). Lingbao Huxin pill alleviates apoptosis and inflammation at infarct border zone through SIRT1-mediated FOXO1 and NF-κB pathways in rat model of acute myocardial infarction. *Chinese Journal of Integrative Medicine*, *28*(4), 330–338. https://doi.org/10.1007/s11655-021-2881-0

Tang, F., & Ling, C. (2019). Curcumin ameliorates chronic obstructive pulmonary disease by modulating autophagy and endoplasmic reticulum stress through regulation of SIRT1 in a rat model. *Journal of International Medical Research*, *47*(10), 4764–4774. https://doi.org/10.1177/0300060519869459

Wang, J., Xu, L. W. J., Tian, L., & Sun, Q. Y. (2021). Circulating microRNA-208 family as early diagnostic biomarkers for acute myocardial infarction: A meta-analysis. *Medicine*, *100*(51), e27779. https://doi.org/10.1097/MD.0000000000027779

Wang, Q., Zhou, H., Zhu, X., Jiang, F., Yu, Q., Zhang, J., & Ji, Y. (2022). miR-208 inhibits myocardial tissues apoptosis in mice with acute myocardial infarction by targeting inhibition of PDCD4. *Journal of Biochemical and Molecular Toxicology*, *36*(12), e23202. https://doi.org/10.1002/jbt.23202

Wei, Y. J., Wang, J. F., Cheng, F., Xu, H. J., Chen, J. J., Xiong, J., & Wang, J. (2021). miR-124-3p targeted SIRT1 to regulate cell apoptosis, inflammatory response, and oxidative stress in acute myocardial infarction in rats via modulation of the FGF21/CREB/PGC1alpha pathway. *Journal of Physiology and Biochemistry*, *77*(4), 577–587. https://doi.org/10.1007/s13105-021-00822-z

Xiao, J., Sheng, X., Zhang, X., Guo, M., & Ji, X. (2016). Curcumin protects against myocardial infarction-induced cardiac fibrosis via SIRT1 activation *in vivo* and *in vitro*. *Drug Design, Development and Therapy*, *10*, 1267–1277. https://doi.org/10.2147/DDDT.S104925

Xie, J. (2023). Long noncoding RNA XIST regulates myocardial infarction via miR-486-5p/SIRT1 axis. *Applied Biochemistry and Biotechnology*, *195*(2), 725–734. https://doi.org/10.1007/s12010-022-04165-3

Xu, X., Shi, Y., Yu, Q., Peng, Y., Zhao, F., Cui, J., Chen, Y., Liu, L., Zhang, Y., Zhang, J., & Wei, B. (2023). Coumarin-derived imino sulfonate 5h ameliorates cardiac injury induced by myocardial infarction via activating the Sirt1/Nrf2 signaling pathway. *European Journal of Pharmacology*, *945*, 175615. https://doi.org/10.1016/j.ejphar.2023.175615

Yamac, A. H., Uysal, O., Ismailoglu, Z., Erturk, M., Celikten, M., Bacaksiz, A., & Kilic, U. (2019). Premature myocardial infarction: Genetic variations in SIRT1 affect disease susceptibility. *Cardiology Research and Practice*, *2019*, 8921806. https://doi.org/10.1155/2019/8921806

Yan, S., Zhou, M., Zheng, X., Xing, Y., Dong, J., Yan, M., & Li, R. (2021). Anti-inflammatory effect of curcumin on the mouse model of myocardial infarction through regulating macrophage polarization. *Mediators of Inflammation*, *2021*, 9976912. https://doi.org/10.1155/2021/9976912

Yang, L., Shi, J., Wang, X., & Zhang, R. (2022). Curcumin alleviates D-galactose-induced cardiomyocyte senescence by promoting autophagy via the SIRT1/AMPK/mTOR pathway. *Evidence-Based Complementary and Alternative Medicine*, *2022*, 2990843. https://doi.org/10.1155/2022/2990843

Yin, Y., Wu, X., Peng, B., Zou, H., Li, S., Wang, J., & Cao, J. (2020). Curcumin improves necrotising microscopic colitis and cell pyroptosis by activating SIRT1/NRF2 and inhibiting the TLR4 signalling pathway in newborn rats. *Innate Immunity*, *26*(7), 609–617. https://doi.org/10.1177/1753425920933656

Zhao, Y., Zhuang, L., Tian, P., Ma, M., Wu, G., & Zhang, Y. (2023). Rapid diagnosis of acute myocardial infarction based on reverse transcription-accelerated strand exchange amplification of miR-208a. *Anal Methods*, *15*(35), 4442–4451. https://doi.org/10.1039/d3ay01116